IEEE Access
Multidisciplinary | Rapid Review | Open Access Journal

Received 18 May 2023, accepted 27 May 2023, date of publication 5 June 2023, date of current version 9 June 2023.

Digital Object Identifier 10.1109/ACCESS.2023.3282729

RESEARCH ARTICLE

PIoT: A Performance IoT Simulation System for a Large-Scale City-Wide Assessment

ABBAS DEHGHANI FIROUZABADI, HAKIM MELLAH, (Member, IEEE), ORESTES MANZANILLA-SALAZAR, (Member, IEEE), REZA KHALVANDI, VINCENT THERRIEN, VICTOR BOUTIN, AND BRUNILDE SANSÒ, (Senior Member, IEEE)

Department of Electrical Engineering, Polytechnique Montréal, Montréal, QC H3T 1J4, Canada

Corresponding author: Abbas Dehghani Firouzabadi (abbas.dehghani@polymtl.ca)

This work was supported in part by the Natural Sciences and Engineering Research Council of Canada (NSERC), and in part by Ericsson under Grant CRDPJ 520642.

ABSTRACT Given the proliferation of sensors and actuators, evaluating the network performance of current and forthcoming city-wide Internet of Things (IoT) applications is a challenging task. To overcome this challenge, we created a large-scale simulator called PIoT over the years that can assess the performance of multiple millions of mobile/static IoT devices using a 4G/5G cellular infrastructure. In PIoT, different Key Performance Indicators (KPIs) are defined and collected to produce data to evaluate applications and network performance. PIoT is an on-going academic simulator project, and its most recent version is accessible to the public through the user interface found on http://www.piotsimulation.com without any installation requirements. It uses a realistic database that contains the real locations and features of Base Stations (BSs) and the real locations of IoT user equipment devices. The interface can be used by operators and researchers to understand network behavior when deploying new applications or to gather data to feed artificial intelligence and machine learning algorithms. The objective of this paper is to present a detailed description of the PIoT modeling architecture, as well as some use cases to help potential users understand the type of capabilities that are available when using the simulator. Limitations and comparisons with other popular engines are also included in the paper.

INDEX TERMS PIoT, large-scale simulator, performance assessment, LTE/5G/B5G networks, data gathering, data mining, key performance indicators.

I. INTRODUCTION

The telecommunication networks of the future will be large-scale connected entities where billions of IoT communications will be happening simultaneously. To analyze and assess the impact of those applications on the infrastructure or on other application behaviors, a city-scale simulator is a primordial tool. Moreover, Artificial Intelligence (AI)/Machine Learning (ML) methods are expanding rapidly, and researchers in this field need data from applications that may not yet be deployed. Therefore, to develop those AI/ML solutions, it is crucial to have a simulator that can provide realistic data on a city scale.

The associate editor coordinating the review of this manuscript and approving it for publication was Nurul I. Sarkar.

To address this need, we developed a large-scale Fourth Generation (4G)/Fifth Generation (5G) city-wide simulator, Performance Internet of Things (PIoT), that can deal with up to multiple millions of mobile/static devices to assess the performance of a city-wide IoT. PIoT has a user-friendly interface that can be found on http://www.piotsimulation.com. The front end is open access and free for everyone to use. In contrast to other simulators, it does not require installation and can be used immediately. Thus, by utilizing this interface, beginners can easily create large-scale scenarios. As an additional benefit, a realistic database that includes information about BSs and IoT devices enhances the users' ability to interact with PIoT. In the current version, the database covers the city of Montreal, but we plan to enlarge the interface so that other cities around the world are covered. PIoT does

not have the time complexity of physical layer simulators. Due to PIoT's modular design, it can be easily extended to implement in other emerging technologies. In contrast, PIoT has some shortcomings: it does not consider the bit error rate and retransmissions, and as it is an on-going project; a number of novel features, such as Integrated Access and Backhaul (IAB), Non-Terrestrial Networks (NTN), and Open Radio Access Network (RAN), moving BSs, etc., have not yet been implemented.

In previous work [1], [2], [3], [4], [5], PIoT was used to simulate communication enabling smart-city applications. However, we have never described in-depth the details of how the simulation is built and what type of features are implemented. Therefore, the motivation for this article is to make that information publicly available so that external users can understand the simulator structure and functionalities. The objective being to provide all the information needed for anyone to adapt PIoT to their simulation needs.

The contributions of the paper can be summarized as follows:

- We describe PIoT modeling architecture in detail, including the access topology, the random access procedure, the packet generation and transmission, the resource scheduling as well as failures, mobility and supplementary elements, such as Narrowband Internet of Things (NB-IoT), network slicing, Multiaccess Edge Computing (MEC) and beamforming. The general features of the simulator are shown in Figure 1.
- We review and classify the literature on popular simulators that can be used to evaluate IoT network performance.
- We present several use cases that can be implemented in our simulator and that can be useful for external users to acquire a better understanding of how PIoT works.

The remainder of the paper is presented as follows. A brief literature review on current simulators is provided in the next section. In Section III, we describe the access topology implementation based on a novel grid structure and show how it relates to a realistic geographical model and databases from the city of Montreal. Section IV depicts a simplified version of the random access procedure implemented in the simulator and shows how to analyze some related KPIs for a large number of devices. In Section V, packet generation and transmission are detailed and scheduling algorithms, channel modeling and Channel Quality Indicator (CQI) (Channel Quality Indicator) computing strategy implementations are discussed. Failures, failure KPIs and recovery profiles are outlined in Section VI. In Section VII, we describe how to implement predefined (i.e. buses, trains, etc.) and random mobility. Handover and mobility KPIs are also discussed in this section. Some supplementary features of the simulator are presented in Section VIII. Section IX concludes the paper.

II. LITERATURE REVIEW

A large body of research has been dedicated to simulating the physical layer of Long-Term Evolution (LTE), such as the MATLAB LTE toolbox [6], [7], [8]. Additionally, a few LTE open-source emulators have been developed in software-defined radio platforms. SRSLTE [9] and OpenAir-Interface [10] frameworks deployed complete functions of user and eNodeB that work on hardware. However, LTE emulators as well as physical layer simulators are appropriate for optimizing the receivers, coding schemes or equalization procedures, not for cell planning, anomaly detection or end-to-end large-scale performance evaluation of the network.

The performance of large-scale cellular networks was studied in [11], [12], and [13] using tools from stochastic geometry. In these studies, a mathematical framework is developed, and theoretical expressions are derived to model and analyze network performance. However, even with simplified forms for a few special cases, there is still a large gap between real world performance and approximated theoretical expressions. Additionally, the mathematical model of dynamic processes, such as resource allocation, handover and failures, are often ignored in studies based on stochastic geometry. They only evaluate the average performance of the network, not the instantaneous performance as a function of time. Recent research on large-scale IoT networks using stochastic geometry techniques has been published in [14]. Based on a spatial distribution model of homogeneous IoT devices, the authors calculate the delay bound of transmissions in some exceptional situations.

Several well-known simulators model IoT applications based on 4G/5G mobile networks, including [15], SimuLTE [16], LTE-Sim [17] and NS-3 [18]. In these engines, the calculations related to the channel model are performed for each User Equipment (UE) and antenna while a change occurs in the network. A comparative runtime analysis (using the NS-3 LTE simulator) for some propagation models is presented in [19]. A key result of that paper is that the computational complexity of the simulation grows rapidly with the number of users and base stations. Additionally, in [20], the computational time for different diffusion propagations is presented. The computation of the path loss models takes approximately 5 μs to 10 μs for each packet in the NS-3 simulator. As a result, it is too difficult to simulate thousands of devices and hundreds of base stations at the scale of a smart city using these types of tools. Furthermore, these simulators do not include real UEs and existing BSs that can be used in the simulation. Moreover, a user's association with each BS must be specified in their configurations. A framework based on NS-3 simulation is presented in [21] for simplifying the evaluation of the performance of an IoT communication technology. In this framework, scenarios are defined, as well as their KPIs and their evaluation. Although these studies simulate more than a thousand devices, they are still insufficiently scalable for large-scale applications throughout a city.

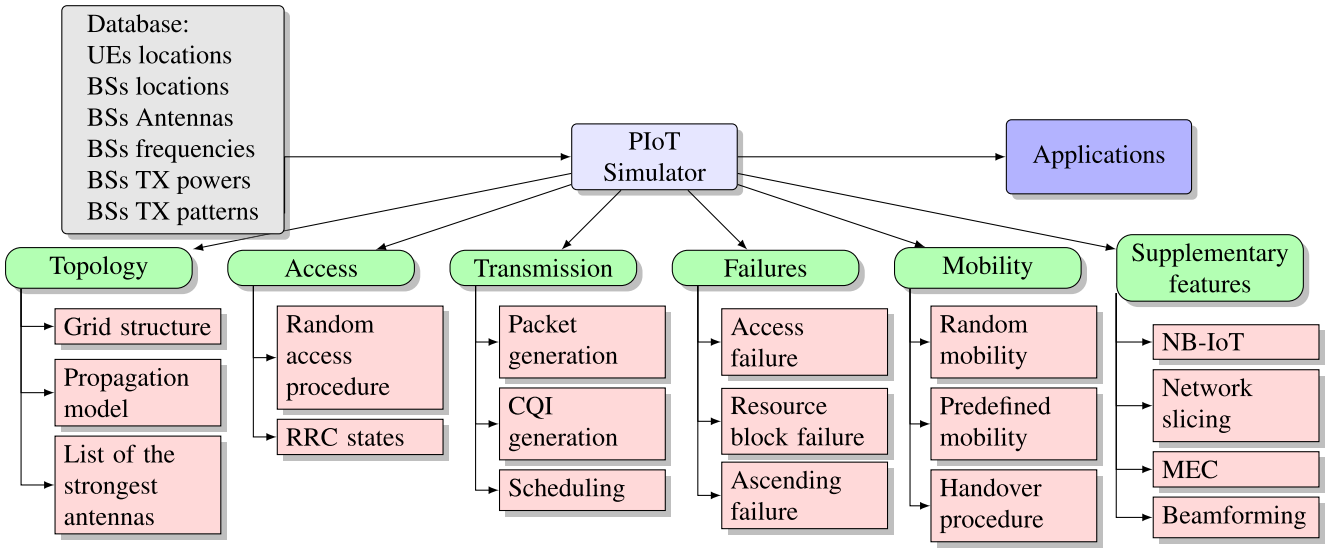

FIGURE 1. General structure of the PIoT simulator.

The control plane latency performance of different NB-IoT optimizations is examined in [22]. Using real hardware, the study was conducted with different packet sizes and levels of coverage. Based on their study, network operators should select the right Transport Block Size (TBS) (Transport Block Size) to avoid resource waste during data transmission. An experimental study of the international roaming performance of NB-IoT networks in Denmark, Sweden and Norway is presented in [23]. By calculating KPIs, such as packet loss, packet delay, and bit rate, they compared the performance of the network at home and on the roaming network. To determine whether IoT technology can support roaming applications, 6000 packets with different payload sizes are sent. In [24] and [25], considering the Internet of Underwater Things, simulations are carried out in terms of energy efficiency, time average age of information, and congestion of network queues. However, they do not consider the LTE/5G network for communication links.

Reference [26] described a scalable smart city simulator in a realistic environment including various types of IoT applications, such as smart buildings, cars, traffic lights, and parking meters in a smart city. This simulator, which can treat multiple IoT nodes in a metropolitan area, is written in the Erlang language because of its efficiency for the massive implementation of multithreading. However, its focus is on the application layer and smart city applications, not on the communication aspects. In fact, InterSCSimulator [26] was a part of a larger project, and it was integrated with [27] to model workload generation in a client-server model. In this paradigm, [26] was responsible for generating smart city requests on the client-server model, and [27] created a platform to simulate smart city applications on the server side. The authors of [28] implemented enhanced machine-type communications (eMTC) and NB-IoT using the NS-3 simulator. Although they showed that using eMTC and NB-IoT in smart city applications can lead to a considerable difference in terms of latency and energy consumption, the simulation scenario is not based on real geographic data. Moreover, despite their simulation of more than a thousand devices in several cells, the approach is not scalable for city-wide applications, and specific mobility models were not designed.

A summary of the literature review is given in Table 1. Although there are many tools that contribute to modeling IoT traffic, there is no comprehensive tool specifically designed to simulate city-wide traffic on a large scale to extract the KPIs of forthcoming applications.

III. GENERAL STRUCTURE AND INITIALIZATION

PIoT is a high-level large-scale simulation system where only user packets are simulated and only at the packet level. Even though the control packets are not simulated, the delay of the control functions is estimated. To date, PIoT has mainly focused on network access to evaluate the effects of IoT devices on wireless access networks. To account for the total delay of the user packets, the core is modeled using logical links. A distribution can be assigned to each of the links to generate a random delay. Thus, an object of Evolved Packet Core (EPC) and Packet Data Network (PDN) is used to generate random delays using a packet delay distribution. There are several BS modules in the radio access network, and antenna modules are assigned to the relevant BS modules. Additionally, various types of UE, including regular, mobile, and NB-IoT, are assigned to each antenna. The main responsibility of the antenna module is resource management. Therefore, several scheduling strategies are implemented. In the UE, the packet generation module simulates different types of IoT applications. With scheduling, CQI, and packet flow, the entire transmission process can be simulated. The random access procedure is also integrated into the UE module.

TABLE 1. Literature review summary table.

References	Approach	Features	Limitations
Our work	Simulation	Simulate multiple millions of devices, Open access user-friendly interface without installation is appropriate for beginners, A realistic database, Time-efficient	Does not include the bit error rate and retransmissions, A number of novel features have not yet been implemented
[6]–[8]	Simulation	Analyses of physical layer algorithms in detail	Network performance evaluation is not included, High execution time for large-scale scenarios
[9], [10], [22], [23]	Hardware implementation	Experimental evaluation	High hardware cost for large-scale implementation
[11]–[14]	Stochastic geometry	Closed-form expressions for a few special cases	Large gap between real-world performance and approximated theoretical expressions
[15]–[18], [21], [28]	Simulation	Network-level performance evaluation	The calculations related to the channel model are performed for each UE and antenna, Difficult to simulate thousands of devices and hundreds of BSs, do not include real UEs and existing BSs
[26], [27]	Simulation	Model workload generation in a client-server model	Focus on the application layer, not the communication aspects
[24], [25]	Simulation	Underwater IoT performance evaluation	No modeling of LTE or 5G network

The general PIoT structure is shown in Figure 1. Realistic BS and UE information, such as type or location, are acquired from the database. Using this information, the topology of the network is provided. A grid structure is considered in which any antenna's received radiation in any grid is calculated by an assisting propagation simulator tool. Then, a UE in any grid is assigned to the most appropriate antenna.

As shown in Figure 1, PIoT access features include the impact of random access procedures and RRC connection states on network performance, such as collisions and RRC delays. The transmission module of PIoT is responsible for generating packets with different distributions, assigning CQI to packets, and scheduling packet resources. Next, by using failure deployment, we can consider any event that disables the antenna or BS partially or completely. Additionally, we can analyze the performance of devices traveling across the city using different mobility deployments. The PIoT simulator now has the capability of adding supplementary features, such as NB-IoT, network slicing, MEC, and beamforming. Each of the elements in Figure 1 is discussed in the following sections.

A. DATABASE

Geographical positions of BSs are provided from the Industry Canada open dataset [29], and the positions of IoT devices are given from a public database [30] that can be related to IoT city applications such as houses, fire alarms, traffic lights, traffic signs, bus stops, pedestrian crossings and security cameras. PIoT considers IoT devices as UEs in each application. Thus, machine types, number of machines and UE mobility are all configurable. Reference [29] also has the BS height, frequency, transmit power and antenna pattern that are used in creating the network topology. In addition, the BS service provider is also given in [29]. Thus, the user has the capability of choosing the cellular operator.

B. TOPOLOGY

City topology is used to calculate signal strength from the antenna considering realistic geographical information. Hence, to simulate the city environment, we extrapolate the city by grids, calculate the power strength from any antenna in the center of each grid, and then provide a list of antennas that produce the strongest signal in any grid. The topology of antennas is derived using realistic data from the city of Montreal [29]. In PIoT, the topology is precalculated and saved as a topology file. A topology file contains information about all BSs in the selected area, such as their latitude, longitude, and antennas. Each antenna in the topology file has information about frequency, bandwidth, and received power for every grid point (determined by latitude and longitude) based on a list of the 12 most powerful antennas. The topology details are given below [31]:

- Grid structure: The city map is divided into square grids called grid points, and the side length of this square can be configured by the user.
- Propagation model: By considering physical and geographical parameters and situations, the propagation model is obtained from 3GPP standards [32], and then the received powers of antennas are calculated in the center of any square.
- List of antennas in each grid point: in any square, we sort the received power from all antennas and choose a list of the N (we have used N=12) antennas with the strongest received power per grid and neglect the others. In Figure 2, we can see an example of how to generate the antenna list. Whenever a UE enters a grid point, it can try to connect to the antenna with the strongest power (the top of the N list). This information is used as a hand over between antennas when there is user mobility, antenna failure, or BS congestion.

C. INITIALIZATION

The initialization process is depicted in Figure 3. At the beginning of the simulator procedure, BS and UE information is loaded from the database, and all grid calculations are loaded from the precomputed topology file. Then, BS and antenna modules are created based on the topology. Next, UE modules are created, and their packets are generated

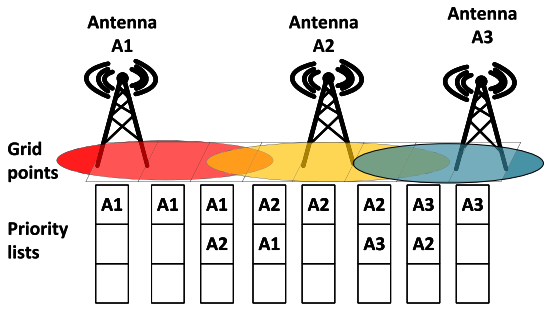

FIGURE 2. Grid points to antenna mapping.

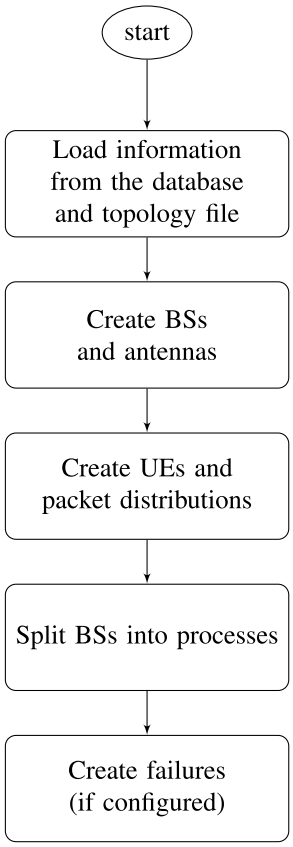

FIGURE 3. Initialization process.

based on the distributions. After that, every UE is assigned to the first antenna from the list assigned to its grid point according to its position. To reduce the simulation execution time, BSs are split into multiple processes. Additionally, failures are created based on the input configurations. The simulation time step is based on a subframe, and the packets are sent or received by the UE according to this time step. Mobility updates are performed for mobile UEs in a time step configurable by the user (1 second by default). If a failure is scheduled in a predefined time, it will be applied in the related time step. Moreover, a handover is executed based on failure or mobility data.

IV. ACCESS

A. RACH (RANDOM ACCESS CHANNEL)

One of the most important access procedures is the RACH attempt. There are two types of RACH attempts: contention-based and contention-free. The first allows the UE to select a random preamble from a pool. If during the attempt, more than one UE chooses the same preamble, a collision happens, a single UE or no UE will be able to connect. On the other hand, the contention-free attempt uses reserved preambles scheduled by the BS to avoid any chance of collision. To use this mode, the UE needs to already be in an RRC_CONNECTED mode [33]. When a UE is in RRC_CONNECTED mode, it is capable of transmitting and receiving traffic data as well as signaling information. This procedure is much shorter because this UE is already known by the network, which avoids much of the setup time.

RACH attempts occur in 6 different cases [34]:

- To connect from RRC_IDLE
- To reconnect after link failure
- To connect to the new cell during handover
- For Uplink (UL) resynchronization upon UL arrival when RRC_CONNECTED
- For UL resynchronization upon Downlink (DL) arrival when RRC_CONNECTED
- For positioning while RRC_CONNECTED

RRC_IDLE, as the name implies, indicates that the UE is powered on, but no RRC connection has been established. We consider that UEs in the RRC_CONNECTED state are always synchronized. Additionally, a RACH attempt during a handover is contention-free, and only the delay during a handover is considered. Thus, in PIoT, the first two cases are considered for the access procedure using a contention-based procedure.

The antenna selection is based directly on the topology generated. At the beginning of the simulation, each UE selects the antenna with the strongest received signal at the current grid point. For mobile UEs, they check if the current connected antenna is in the list of the new grid point. If not, it searches for an antenna from the same BS. When no antennas from the currently connected BS are present, the antenna with the strongest received signal is selected and a handover procedure is carried out. See section VII for more details.

In practice, RACH attempts consist of 4 messages: the random access preamble, the random access response, the scheduled transmission and the contention resolution. The first message is sent by the UE to initiate the RACH attempt. The second message is sent by the BS to assign UL resources for the next transmission. The third consists of RRC signaling from the UE. In addition, the final one is a contention resolution, which confirms the successful connection or not [34].

For the simulator, the main concern is to detect a collision and apply an appropriate delay. Therefore, the connection process is modeled by a delay. In LTE, two RRC states are allowed: idle and connected. A UE needs to be in the connected mode to send or receive packets. Therefore, a UE

in idle mode needs to make RACH attempts when a packet is generated or paging indicates an incoming DL packet. For ease of simulation, another state is defined in the simulator, which is *connecting*. UEs enter this state when they attempt to connect, and they exit it after the connection delay, regardless of whether the connection is successful or not. At the beginning of the connection, a preamble is chosen. If more than one UE uses the same preamble at the same time, a flag is raised to indicate a collision. At the end of the connection delay, if the collision flag is set, the UE is set to idle; otherwise, it is set to connected. When a UE is set back to idle after a collision, it waits a random time between 1 and the backoff indicator in milliseconds before attempting another connection. The scenario where one UE dominates the other during a collision and is successfully connected is excluded.

To isolate machine-type communication from human-type communication, resources can be distributed as explored in [35]. Thus, the number of available preambles can be set. Additionally, the PRACH configuration index must be assigned manually to applications in the configuration file. According to [36], the access delay for LTE is, on average, approximately 50 ms. In the simulator, this value is set by the user, and two strategies can be used, constant delay or random delay, which are distributed uniformly within a set margin of error.

In 5G networks, to minimize latency and signaling overhead, a new connection state was introduced, the RRC_INACTIVE state [5]. In this state, UE retains the RRC context for a period of time. Thus, the time for transition from the inactive state to the connected state is considerably reduced. As mentioned earlier, the access delay takes approximately 50 ms. Due to the reduced signaling overhead on the core side, only a few steps are required to enter the connected state, approximately 20 ms. In the simulator, this connection time can be preset by the user.

B. KPIs FOR RACH

Three categories of KPIs are produced by the simulator for the RACH. The first category is the attempt KPIs, which record the number of attempts and failed attempts. The second category is the collision KPIs, which count the collisions and give a ratio of collisions to transmissions. The last category is the delay KPI that measures the connection delay. The KPIs are defined in Table 2.

C. SAMPLE SIMULATION RESULTS

In this paper, we performed all simulations for the whole city of Montreal with 343 BSs. To observe the impact of simulation parameters on the RACH KPIs, 4 scenarios are explored. All of them have two LTE applications in common, pedestrian crossings and traffic lights, including 310,000 devices. They send packets at mean rates of 0.5 and 1 packet per second using an exponential distribution. The simulation duration is 5 minutes, and all UEs are assumed to be connected at the start. Parameters specific to the four different scenarios are shown in Table 3.

TABLE 2. RACH KPIs.

KPI	Description
Total RACH Attempts	Total number of RACH procedures attempted.
Total Failed Rach Attempts	Total number of RACH procedures failed.
Collision Count	Number of collisions experienced (counted for each UE in a collision).
Collisions Transmissions Ratio	Ratio between the number of collisions and the total number of RACH attempts.
RRC Delay	Time between the moment a UE tries to connect and the time it is successfully connected.

TABLE 3. RACH parameters.

Scenario	PRACH index (app1, app2)	Number of available preambles
1	(0, 0)	20
2	(0, 0)	5
3	(1, 0)	5
4	(14, 14)	5

TABLE 4. RACH KPIs.

Scenario	Total RACH attempt	Collision ratio	RRC Mean Delay (ms)
1	1 078 725	0.0086	50.9134
2	1 099 920	0.0308	53.4036
3	1 084 783	0.0152	51.6578
4	1 085 474	0.0015	50.1614

As shown in Table 4, the variation of the PRACH index and the number of available preambles affect the collision rate and RRC access delay. First, there is a relation between the collision ratio and the RRC delay. When a collision occurs, the RRC connection is prolonged for at least a backoff time. and another random access is attempted. Second, collisions are inversely proportional to the number of available preambles. Third, the PRACH index plays an important role in the collision ratio. The PRACH index parameter specifies the frame number and subframe number the UE can send the RACH preamble. PRACH index 14 allows the UE to send the preamble in any frame and any subframe [37, Table 5.7.1-2]. An application with a restrictive index (e.g., index 0) and/or an index shared with another application will be more likely to have a collision. However, a permissive index (e.g., index 14) will allow fewer collisions.

V. TRANSMISSION

A. PACKET GENERATION DISTRIBUTIONS

Machine-type traffic is a broad term regrouping machine generated traffic without human interaction. The traffic patterns of machines are considerably different from those of humans [38]. For example, in [39], packet interarrival time is considered uniform (not synchronized) or beta (synchronized). This traffic diversity requires high flexibility in packet generation

TABLE 5. Random distributions implemented.

Distribution	Parameters
beta	-alpha: α parameter -beta: β parameter -scale: Defines the range of generation ([0,scale])
constant	constant_value: Value generated
exponential	-scale: Average time (in ms) between packets (Inverse of the rate parameter λ)
gamma	-k: Shape parameter -theta: θ parameter
log_normal	-s: σ parameter -scale: Scale parameter
uniform	-min: Minimum value of the generation interval -max: Maximum value of the generation interval
weibull	-c: Shape parameter -scale: Scale parameter

TABLE 6. CQI computation strategies and parameters.

Computation Strategy	Parameters
Identical	-IdenticalCQI: Constant CQI.
Random	-MinimumCQI: Minimal possible CQI value. -MaximumCQI: Maximal possible CQI value.
Distance Dependent	-Minimum Distance: Distance from antenna associated with the minimum CQI. -Maximum Distance: Distance from antenna associated with the maximum CQI. -MinimumCQI: Minimal possible CQI value. -MaximumCQI: Maximal possible CQI value.
Power Dependent	-Minimum Power: Received power from antenna associated with the minimum CQI. -Maximum Power: Received power from antenna associated with the maximum CQI. -MinimumCQI: Minimal possible CQI value. -MaximumCQI: Maximal possible CQI value.

that is defined by two distributions. One describes the length of the packet, while the other describes the interarrival time. The available distributions are presented in Table 5.

In the simulator, packets are pregenerated at the start of the simulation, before the discrete events. To generate the random values, the Python module, Scipy, is used. The user may generate multiple applications with different packet generation, UE distribution and traffic direction (i.e., UL or DL). For UL, during the discrete event runtime, when the subframe of creation is processed, the UE initiates the RACH procedure (if needed) and then sends the packet to the scheduler to assign time-frequency resources. For DL, a similar process occurs, but packets are sent from the network to the UE.

B. SCHEDULING

In 4G/5G networks, the time-frequency resource unit is a Resource Block (RB). An RB spans a subchannel (12 subcarriers) in specified time symbols. This determines the simulator's smallest timestep [40]. Variable SCS (Subcarrier Spacing) is a new feature in 5G. In LTE, there is only one subcarrier spacing, 15 kHz. In 5G, one can choose multiple different types of subcarrier spacing, 15, 30 and 60 kHz in frequency range 1 and 60 and 120 kHz in frequency range 2. SCS can be chosen in the simulator by the user.

Using the data from the real antenna, the position and bandwidth used by the antenna are determined. The bandwidth can then be converted into a number of RB available for transmission by a subframe. A fraction of these RBs can be selected for UL and DL transmissions in the parameter entry. The separation of RB for UL and DL makes it possible to process the UL and DL scheduling independently.

The implemented scheduler abstracts the signaling. Each antenna has an associated scheduler. Once a packet is ready for transmission (i.e., connected state and a packet is generated), the packet is sent to the scheduler. The scheduler assigns a priority to each packet depending on the applied strategy. Then, the scheduler attributes RBs to the packets until there is no packet left, or there is no RB in the scheduling subframe.

Multiple scheduling techniques are implemented in the simulator based on strategies described in [40]:

- First In First Out (FIFO): Packets are scheduled in the order of arrival.
- Last In First Out (LIFO): Packets with the lowest age are prioritized.
- Round Robin (RR): Packets generated by UEs that have not been transmitted for a long time are prioritized.
- Blind Equal Throughput (BET): Packets with the lowest average throughput are prioritized.
- Maximum Throughput (MT): Packets that have the highest possible throughput (i.e., the number of possible transmission bits to the required resources) are prioritized.
- Proportional Fair (PF): Similar to BET but weighted with the maximum throughput.

To determine the number of RBs needed for a transmission, the TBS (Transport Block Size) must be considered. To model the channel quality, a channel quality indicator (CQI) is assigned to each UE and is refreshed periodically with a period set by the user. The CQI is defined by the user per application with options shown in Table 6. For random CQI generation, the random distribution is uniform between the maximum and minimum parameters. In the case of distance power-dependent and power-dependent CQI generation, linear interpolation is used to determine the CQI by associating the minimal CQI with the minimal received power and distance from the antenna and the maximal CQI with the maximal received power or distance from the antenna. If a distance or power value falls below the minimal value, the CQI is minimal, and the same is true if the maximum value is exceeded.

To calculate the TBS from the CQI, the Modulation and Coding Scheme (MCS) index is considered a linear function of the CQI. The TBS is linked to the MCS via tables found in the standards [41]. The TBS determines the quantity of data that can be sent depending on the number of RBs used.

TABLE 7. Transmission KPIs.

KPI	Description
Total Created Packets	Total number of packets created by all UEs.
Total Transmitted Packets	Total number of packets transmitted from the UEs to the network.
Total Traffic	Total volume of traffic transmitted (in bits).
Total Transmission Time	Total time spent transmitting.
Used Resource Blocks	Number of resource blocks used for packet scheduled in the period.
Used Resource Blocks Percentage	Ratio of used resource blocks on available resource blocks.
Throughput	Ratio of the volume of data transmitted by the transmission time (aggregation).
Transmission Delay	Time between the transmission of the first bit to the reception of the last bit (aggregation).
Waiting Delay	Time between the packet creation and the transmission of the first bit (aggregation).

TABLE 8. Transmission parameters.

Scenario	Generation distribution (length, interarrival)	CQI	Direction
1	Exponential (1000, 250)	[5-15]	Uplink
2	Beta (1000, 250)	[5-15]	Uplink
3	Exponential (1000, 250)	[1-10]	Uplink
4	Exponential (2000, 250)	[5-15]	Uplink
5	Exponential (1000, 125)	[5-15]	Uplink
6	Exponential (1000, 250)	[5-15]	Downlink

C. KPIs FOR TRANSMISSION

The transmission module provides a rich variety of KPIs for generation, resource usage and various delays. These KPIs are described in Table 7.

These KPIs can be separated into two categories. The first category is the global KPIs that provide an overview in terms of quantities. These KPIs are the ones prefixed with ''total'' and ''used resource blocks''. The second category is the packet based KPIs that provide statistical information on the quality of the transmission that includes the delays and the throughput.

D. SAMPLE SIMULATION RESULTS

To explore the capabilities of the simulator, two different tests are presented here. The first uses different scenarios in which the generation distribution, the CQI and the direction (UL or DL) varies. The second shows the scheduling effect by using a scenario with congestion and by changing the scheduling strategy. Both are based on security camera locations that include 430 devices. The simulation duration is 1 minute.

Table 8 shows the different parameters used for each scenario. The global results are given in Table 9. They reflect the chosen distribution parameters as well as the remaining traffic in the queue by considering the difference between the packets created and the packets transmitted. Even though the CQI value was greatly reduced in scenario 3, the amount of total traffic is relatively unchanged compared to that in scenario 1.

TABLE 9. Transmission global KPIs.

Scenario	Created Packets	Transmitted Packets	Total Traffic (bit)
1	103 976	103 940	835 739 744
2	103 285	103 261	825 457 288
3	103 976	100 836	810 200 448
4	103 978	103 897	1 669 989 152
5	205 899	205 797	1 644 517 704
6	104 046	103 908	832 121 836

TABLE 10. Transmission packet KPIs (average).

Scenario	Throughput (kbps)	Transmission Delay (ms)	Waiting Delay (ms)
1	775.679	13.2118	22.4647
2	777.9128	13.124	18.8539
3	351.1899	56.0734	1943.3168
4	832.9019	25.869	53.6354
5	766.9791	13.1354	28.1537
6	771.9152	13.1683	22.7068

The packet results in Table 10 show the differences between the simulation scenarios. Most parameters do not affect the throughput and the transmission delay. The exceptions are the size of the packets and the CQI. The CQI is greatly reduced in scenario 3, which impacts the throughput and transmission, causing congestion and greatly increasing the waiting delay. Furthermore, considering the same number of transmitted bits (i.e., interarrival time $\times$ packet length), scenario 4, which generates packets with a longer length (2000), provides worse performance than scenario 5, which generates more packets with a shorter length (1000).

In another evaluation, we analyze two uplink applications that compete for the same resources. In both applications, the number of transmitted bits is the same, and packet lengths and interarrival times are distributed exponentially. However, application 1 sends packets of 1000 bits on average compared to the 200 bits for application 2. The CQI is considered constant to reduce the random factor. The results are shown in Table 11. For each scheduling row, the results for applications 1 and 2 are presented.

In FIFO scheduling, we can see that there is almost an equal waiting delay for applications 1 and 2. Therefore, in this strategy, the size of the packets has no effect on the priority given to the packets of both applications. In the LIFO, BET and PF strategies, the waiting delay for application 2 with smaller packets is better than that for application 1 with larger packets. In contrast, the RR and MT schedulers provide the advantage to application 1. Moreover, we can observe that the difference between the throughput of applications 1 and 2 is the lowest in BET scheduling and the highest in MT scheduling.

VI. FAILURES

Failure modeling is the study of outage effects, as well as their detection, compensation, diagnosis and restoration of the system's normal functionality. In the context of this paper,

TABLE 11. Scheduling impact on KPIs.

Scheduling Strategy	Transmitted Packets	Total Traffic (bits)	Throughput (kbps)	Waiting Delay (ms)
FIFO	96 141 472 182	772 463 088 757 280 624	161.205 140.2636	1689.3841 1637.0693
LIFO	91 668 492 286	690 907 872 761 377 616	158.1358 139.9462	907.9618 412.4055
RR	102 518 440 548	823 788 160 706 607 168	157.3886 137.3516	420.9036 1803.9481
BET	97 004 467 556	779 902 304 749 704 808	146.8177 139.6687	1190.5726 987.1218
MT	93 357 487 620	749 200 616 780 189 960	161.645 139.7292	876.007 1046.8502
PF	96 015 472 633	777 561 712 758 092 008	153.4242 139.2549	1007.8548 766.8213

we do not distinguish between the terms failure, fault and outage, as we globally refer to ''failure'' as any event in which an antenna or BS function are partially or totally disabled.

A. FAILURE TYPES

In the literature, the most common strategies to model or simulate failures are as follows:

- Transmit power or antenna gain is totally or partially attenuated [42], [43], [44], [45], [46], [47], [48], [49].
- Access attempts are set to fail [3], [4], [50], [51]
- Direct reduction of transmission bit rate [52]
- Omission or shut down of the BS [53]

In PIoT, three failure types are considered:

1) *Access failures:* the Random Access Channel (RACH) procedure fails, forcing devices requesting a new connection to send their access requests to another antenna or BS. This failure model is useful to replicate the effects of the ''sleeping cells'' [4], [43], [44], [45], [46], [50], [51], [54], [55], as ongoing transmissions and devices with an active connection continue to be served.
2) *Resource block failures:* a fraction of the resource blocks are made unavailable for data transmission in an antenna or BS. In addition to being useful for modeling software malfunctions or configuration problems, this type of failure can also be used to model congestion caused by resources used by background traffic. This failure definition is new. In the literature, the transmission rate has been used to model failures [52], but to the best of our knowledge, no previous work has proposed a failure by using resource blocks.
3) *Ascending Failures:* This type of failure only affects resource blocks, and its severity is not constant. As shown in Figure 4, there is an ascending duration before the failure is stable and reaches the specified severity. It also takes some time to return to zero after the stable duration. Hence, this type of failure has three time durations: the stable duration, which is the number of subframes in which the severity is at its peak; the ascending duration, which is the time taken to go from zero to the specified severity; and the descending duration, which is the time taken to go from the specified severity back to zero. In the failure parameters, we only need to specify the total duration of the failure, the stable duration and the ascending duration since the descending duration can be calculated from the previous three.

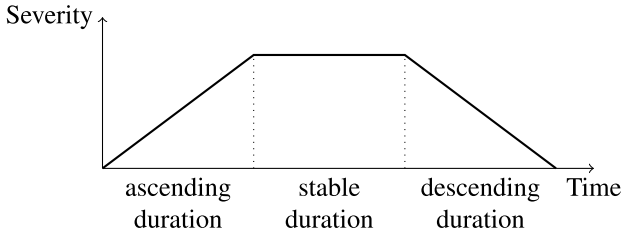

FIGURE 4. Ascending failure.

There are three ways in which the three types of failures can be parameterized:

- *Randomness:* The three types of failures can be specified in a deterministic way, in specific antennas, BSs, and time intervals, or their occurrence and duration can be considered a random variable with parameters defined by the user.
- *Severity:* failures of resource blocks can be defined as partial or total. Severity is the percentage of unavailable resource blocks.
- *Level:* Failures may be defined to take place at the antenna or BS level. BS-level failures occur simultaneously in all the antennas of the BSs, while antenna-level failures are defined for specific antennas in the network.

Randomness, severity and level of failures can be defined in any combination, allowing the practitioner to create scenarios according to the goal of their research. Random failures, for example, can be used when considering failures that occur because of random malfunctions. However, specific deterministic failures can follow a variety of patterns according to user requirements. For an example, we consider the case of an area-wide outage because of a partial energy black-out in the city or the case of an earthquake or a fire affecting a region of the city. The user can use information from another simulator that determines which areas are affected to make the BSs of those regions fail. As deterministic failure times of start and duration are provided by the user, it is possible to simulate progressive spread of the outage of the BSs through the city or any other dynamic of appearance of the failures.

B. KPIs FOR FAILURES

The following indicators have been implemented to measure the impact of failures on the network's performance:

- Total packets affected by failures: Total number of packets that are affected during the failure.
- Total failed RACH attempts: The definition is given in Section IV.

Note that other KPIs previously mentioned can also show the effect of failures.

TABLE 12. Failure parameters.

Scenario	Failure type	Failure duration
1	Access	10 second
2	Resource block	10 second
3	Ascending	10 second

TABLE 13. Failure KPIs.

Scenario	Total failed RACH attempts	Total packets affected by failures
1	4796	0
2	0	215
3	0	45680

C. SAMPLE SIMULATION RESULTS

We consider three scenarios to illustrate the effect of various types of failures on the KPIs and an LTE application using 335190 houses as UEs. UEs generate packets at a mean rate of 1 packet per second using an exponential distribution. The simulation duration is 2 minutes. Failures are assumed to occur from the beginning in all antennas of 20 BSs randomly selected from 343 BSs. We assume 100 percent severity for scenario 2. Additionally, in scenario 3, after the ascending duration, failure reaches 100 percent severity for the stable duration. In this scenario, the stable duration is 2 seconds and both the ascending and descending durations are 4 seconds. Other simulation parameters related to scenarios are shown in Table 12.

As shown in Table 13, in scenario 1, we have 4796 failed RACH attempts in all BSs. After 3 failed RACH attempts, the UE devices try to connect to the next BS from which they receive more power. In scenario 2, because of the full resource block failure, the UE cannot send packets. Thus, after waiting for the maximum waiting delay (200 ms), the UE devices decide to connect to the other BS. Only 215 packets are affected by this failure. In scenario 3, there is a partial failure on resource blocks during the ascending time. Therefore, at this time, UEs have the opportunity to send their packets. As a result, in the end, more packets are affected by the failures than in scenario 2. In the stable time, there is a full failure on resource blocks until the beginning of the descending failure time. Hence, the UE devices decide to connect to the other BSs due to a large waiting delay.

VII. MOBILITY

Mobile user equipment can be included in simulations to analyze the performance of devices that travel around the network. Mobility-related procedures have been based on the 3GPP specifications.

A. MOBILITY TYPES

During a simulation, mobile devices travel across the topology by following itineraries defined as sequences of *locations*. Each location is represented as a coordinate (in latitude and longitude) and a time at which it is reached by a mobile device. Itineraries can be defined in two different ways.

1) RANDOM

Itineraries can be generated randomly at the beginning of a simulation by using three parameters: the *interarrival time* (the time required to travel between two locations), the *interarrival distance* (the distance between two locations), and the *interarrival random factor* (a number that randomly varies the interarrival distance).

Itineraries are created from an initial location by randomly selecting a range of valid *directions* within two radii. Subsequent locations are obtained from the three parameters and the travel direction.

This operation generates unique itineraries composed of locations distributed around a straight line. If the line goes out of the simulation's boundary, the direction is changed to generate other valid locations. This generation method ignores real elements of the city (roads, physical obstacles, etc.) and does not realistically portray how devices travel in a network.

2) PREDEFINED

Itineraries can be described in JSON files that contain location sequences. The simulator assigns these locations as trajectories to devices of a mobile application. Any correctly formatted file (i.e., whose locations are within a simulation topology) can be used to model trajectories.

Two such files have been created from data generated by buses of the STM (Montreal public transit society). They provide an accurate representation of how real life equipment travels in an urban environment. Itineraries for business days and weekends can be used.

B. HANDOVER

A handover procedure is used by mobile devices when they change the base station to which they are connected for a nearer station to improve signal reception. This process has been implemented in the simulator following the norms defined by 3GPP.

A device attempts a handover when the signal of the base station to which it is connected becomes no longer available at the location of a device. The device performs a *contention-free RACH attempt* to establish a connection with the base station that offers the highest signal quality in the region in which the device is currently located. Since resources are allocated in advance for the handover by the two participating base stations, no collision with other connecting devices is possible. However, if the base station that a UE tries to connect to experiences a failure, the handover is unsuccessful.

In reality, the two base stations participating in the handover exchange signals to coordinate device connection transfer. This process is not considered in the simulator.

C. KPIs FOR MOBILITY

The following indicators are specific to mobile applications and serve to analyze their performance.

TABLE 14. Mobile simulation results, random itineraries.

Speed	Handover	Visited Cells	Total Delay (ms)
0 m/s	0	0	115.7
6 m/s	75	56,111	131.1
12 m/s	83	58,182	134.1

TABLE 15. Mobile simulation results, predefined itineraries.

Application	Handovers	Visited Cells	Total Delay (ms)
Static Devices	0	0	136.7
Moving Buses	94	1123	299.1

- Handover count: The number of contention-free RACH attempts performed during handovers. Handovers are recorded by the antennas that offer connection to an incoming mobile device.
- Number of visited cells: The number of times that mobile devices enter regions covered by base stations to which they are not connected. This KPI provides an indication of how mobile devices are traveling; a low number indicates that devices tend to remain in the same cell.
- Handover failure count: The number of times that handovers failed because a device attempted to connect to a nonoperating base station.

D. SAMPLE SIMULATION RESULTS

The following simulation results illustrate the effect of mobility on the performance of applications.

1) FIRST SET, RANDOMLY MOVING DEVICES

Three simulations were performed. Each is composed of an application made of 1,000 devices that simulate background traffic and one mobile application with 500 devices. Packets are generated following an exponential distribution; they are sent each second for background traffic and twice each second for the mobile application. Devices are distributed evenly across the simulation topology. The uplink data rate is determined by using the power received from a base station. Simulations last five minutes, and the first sixty seconds are not included in the result compilation. The speed of mobile devices is the only parameter that varies across simulations.

When the device speeds increase, more cells are visited and additional handovers are recorded because devices travel away from their corresponding base station. Additionally, uplink data transmissions are on average longer than with static devices because mobile devices are not connected at all times to the optimal base stations. At the beginning of a simulation, all devices select the base station that offers the best connectivity (i.e., the highest power), but as devices travel to other locations, the received power decreases, which lowers the CQI, and thus, the data rate. This contrasts with static devices, which are connected at all times to an optimal base station. Other sources of delay, such as RACH procedures and scheduling, are not affected by mobility. Hence, the simulator measures which parts of data transmission are most affected by mobility.

2) SECOND SET, REALISTIC MOTIONS

The trajectory of real applications (public transit buses) are used to portray realistic motions that take the actual topology of the city into consideration. Two simulations were performed: one with the position of buses at noon and the other with moving devices that follow bus itineraries during a working day. Other parameters are the same as those in the preceding simulation set.

The same observations are made: the uplink data rate decreases when devices are moving while access and scheduling-related delays are unaffected. The difference between static and mobile devices is more drastic than with the other simulation set because most buses are located in high-density regions. Thus, shorter travels are more likely to decrease channel quality. Therefore, real life trajectories yield specific results on how they affect the network performance of an application.

VIII. SUPPLEMENTARY FEATURES

This section presents supplementary features that have either been published in a separate work or are in development within the simulator.

A. NB-IoT

NB-IoT is a radio technology standard designed to connect densely located indoor devices requiring long battery life. Despite having modest individual data capacity, these devices can generate a large amount of traffic that strains the communications network. Reference [56] describes NB-IoT features of the simulator in detail.

B. NETWORK SLICING

One way to build a private network within a public network infrastructure is by using network slicing. For example, it may enable the military to use a slice of public 5G infrastructure as a dedicated private-like infrastructure for tactical use [57]. Slicing RAN resources can be accomplished by time, frequency, beam, code, hardware equipment, and other dimensions [58]. Due to bounded RAN resources, we must guarantee that users are able to overcome that limitation and communicate without running into any issues.

In the simulator, two aspects of network slicing are considered [5]. First, we can allocate a fraction of RAN resources to a specified slice. Thus, there are reserved resource blocks for the applications associated with the slice. Second, it is possible to specify a core delay for the slice that can be modeled by a random distribution. Therefore, each slice has a certain delay for the packets passing across the core network. Other details of network slicing are currently in the process of implementation.

C. MULTIACCESS EDGE COMPUTING

MEC, which offers cloud computing services to users, is a useful method for reducing latency in Machine-to-Machine (M2M) applications. Instead of using the core network, the user connects directly to the cloud edge hosts. Additionally, BS-level MEC development will lessen bottlenecks and system failures [59].

To maintain optimal performance in a dynamic environment, it is essential for IoT devices to exchange knowledge and data about the surrounding environment in real-time [60]. Consequently, in the simulator, we assume that the edge host servers are located close to the BSs. Edge application packets do not pass through the core network. Hence, these users will experience less network latency.

D. BEAMFORMING

Massive Multiple-Input-Multiple-Output (MIMO) along with beamforming is one of the key features in 5G due to its increasing spectral efficiency [61]. To enhance the signal strength and data rates for end-users, beamforming technique is commonly employed [62]. Reliable communication and low complexity signal processing are the main advantages of massive MIMO systems. Using beamforming, multiple users can send data packets on the same RB in semiorthogonal channels. The simulation of beamforming gives the ability to obtain more insights into the design and analysis of the network. In the simulator, we consider the semiorthogonality channel condition in [63] for scheduling a user's packets by the same RB. The number of orthogonal beams can be set by the user. As a result, when beamforming is used in the BSs, we observe a clear KPI improvement.

IX. CONCLUSION

Networks of the future will have to respond to society's growing need for flexibility and stringent applications, which means that intelligent system automation will continue to grow through massive M2M and IoT large-scale deployment. For operators to be able to assess the network impact of those forthcoming applications, large-scale simulators are needed. To respond to that need, we developed a simulator system that encompasses a front end, a simulation backend and geographical and application databases. The system, PIoT, is available to the public at www.piotsimulation.com. In this paper, we described each of PIoT's major features and limitations in detail so that potential users would be able to assess its suitability for their own needs. PIoT allows us to test how well a single or group of applications will perform in a realistic 4G/5G city-wide setting and allows the user to extract KPI data that can be used to develop AI and ML algorithms before application deployment. PIoT is an ongoing project, so, given the rapid telecommunication changes, several enhancements are being researched and implemented. First, while the grid that results from our propagation engine is currently given as an entry for the simulator, the user may be interested in changing propagation features on the fly. Therefore, we are planning to add that engine to the public website, and we are currently studying the most efficient way for this to be integrated into the system. Second, there are a number of developments being announced by the 3GPP that we are planning to incorporate into the simulator. Among them, nonterrestrial BSs account for connections to satellite networks, and IAB systems increase backhaul flexibility. Third, IoT applications of the future, such as V2X or the metaverse, will be much more stringent and complex, requiring the interaction of several, sometimes largely distributed, user equipment. We are currently modeling those types of applications and studying their efficient implementation in the PIoT. Another important aspect that cannot be overlooked is the pervasive influence of virtualization on the network. Thus far, those aspects have not been directly accounted for, but they should be more detailed in future edge and core simulation developments.

REFERENCES

[1] F. Malandra and B. Sansò, "A simulation framework for network performance evaluation of large-scale RF-mesh AMIs," *Simul. Model. Pract. Theory*, vol. 75, pp. 165–181, Jun. 2017. [Online]. Available: http://www.sciencedirect.com/science/article/pii/S1569190X17300734

[2] F. Malandra and B. Sanso, "A simulation tool for the performance evaluation of large-scale RF-mesh networks for smart grid and IoT applications," in *Proc. 1st EAI Int. Conf. Smart Grid Assist. Internet Things*, Jul. 2017, pp. 54–63.

[3] F. Malandra, L. O. Chiquette, L.-P. Lafontaine-Bédard, and B. Sansò, "Traffic characterization and LTE performance analysis for M2M communications in smart cities," *Pervas. Mobile Comput.*, vol. 48, pp. 59–68, Aug. 2018.

[4] O. Manzanilla-Salazar, F. Malandra, and B. Sansò, "ENodeB failure detection from aggregated performance KPIs in smart-city LTE infrastructures," in *Proc. 15th Int. Conf. Design Reliable Commun. Netw. (DRCN)*, Mar. 2019, pp. 51–58.

[5] V. Boutin, H. Mellah, C. Wetté, and B. Sansò, "Simulating large-scale 5G networks," in *Proc. IEEE 4th 5G World Forum (5GWF)*, Oct. 2021, pp. 293–298.

[6] I. The MathWorks. (2022). *LTE Toolbox*. Natick, Massachusetts, United State. [Online]. Available: https://www.mathworks.com/help/lte

[7] C. Mehlführer, M. Wrulich, J. C. Ikuno, D. Bosanska, and M. Rupp, "Simulating the long term evolution physical layer," in *Proc. 17th Eur. Signal Process. Conf.*, Aug. 2009, pp. 1471–1478.

[8] C. Bouras, G. Diles, V. Kokkinos, K. Kontodimas, and A. Papazois, "A simulation framework for evaluating interference mitigation techniques in heterogeneous cellular environments," *Wireless Pers. Commun.*, vol. 77, no. 2, pp. 1213–1237, Jul. 2014.

[9] I. Gomez-Miguelez, A. Garcia-Saavedra, P. D. Sutton, P. Serrano, C. Cano, and D. J. Leith, "SrsLTE: An open-source platform for LTE evolution and experimentation," in *Proc. 10th ACM Int. Workshop Wireless Netw. Testbeds, Exp. Eval., Characterization*. New York, NY, USA: Association for Computing Machinery, Oct. 2016, pp. 25–32, doi: 10.1145/2980159.2980163.

[10] R. Wang, Y. Peng, H. Qu, W. Li, H. Zhao, and B. Wu, "OpenAirInterface—An effective emulation platform for LTE and LTE-advanced," in *Proc. 6th Int. Conf. Ubiquitous Future Netw. (ICUFN)*, Jul. 2014, pp. 127–132.

[11] M. Gharbieh, H. ElSawy, A. Bader, and M. Alouini, "Tractable stochastic geometry model for IoT access in LTE networks," in *Proc. IEEE Global Commun. Conf. (GLOBECOM)*, Dec. 2016, pp. 1–7.

[12] J. G. Andrews, F. Baccelli, and R. K. Ganti, "A tractable approach to coverage and rate in cellular networks," *IEEE Trans. Commun.*, vol. 59, no. 11, pp. 3122–3134, Nov. 2011.

[13] H. S. Dhillon, R. K. Ganti, F. Baccelli, and J. G. Andrews, "Modeling and analysis of K-tier downlink heterogeneous cellular networks," *IEEE J. Sel. Areas Commun.*, vol. 30, no. 3, pp. 550–560, Apr. 2012.

[14] M. Mei, M. Yao, Q. Yang, M. Qin, Z. Jing, K. S. Kwak, and R. R. Rao, "On the statistical delay performance of large-scale IoT networks," *IEEE Trans. Veh. Technol.*, vol. 71, no. 8, pp. 8967–8979, Aug. 2022.

[15] J. Colom Ikuno, M. Wrulich, and M. Rupp, "System level simulation of LTE networks," in *Proc. IEEE 71st Veh. Technol. Conf.*, May 2010, pp. 1–5.

[16] A. Virdis, G. Stea, and G. Nardini, "SimuLTE—A modular system-level simulator for LTE/LTE-A networks based on OMNeT++," in *Proc. 4th Int. Conf. Simul. Model. Methodologies, Technol. Appl. (SIMULTECH)*, Aug. 2014, pp. 59–70.

[17] G. Piro, L. A. Grieco, G. Boggia, F. Capozzi, and P. Camarda, "Simulating LTE cellular systems: An open-source framework," *IEEE Trans. Veh. Technol.*, vol. 60, no. 2, pp. 498–513, Feb. 2011.

[18] N. Baldo, M. Miozzo, M. Requena-Esteso, and J. Nin-Guerrero, "An open source product-oriented LTE network simulator based on ns-3," in *Proc. 14th ACM Int. Conf. Model., Anal. Simul. Wireless Mobile Syst.*, Oct. 2011, pp. 293–298.

[19] S. Mohanty and S. Mishra, "Performance evaluation of wireless propagation models for long term evolution using NS-3," in *Proc. Int. Conf. Man Mach. Interfacing (MAMI)*, Dec. 2015, pp. 1–5.

[20] M. Stoffers and G. Riley, "Comparing the ns-3 propagation models," in *Proc. IEEE 20th Int. Symp. Model., Anal. Simul. Comput. Telecommun. Syst.*, Aug. 2012, pp. 61–67.

[21] S. Si-Mohammed, T. Begin, I. G. Lassous, and P. Vicat-Blanc, "ADIperf: A framework for application-driven IoT network performance evaluation," in *Proc. Int. Conf. Comput. Commun. Netw. (ICCCN)*, Jul. 2022, pp. 1–8.

[22] D. Segura, E. J. Khatib, J. Munilla, and R. Barco, "NB-IoT latency evaluation with real measurements," in *Proc. IEEE Workshop Complex. Eng. (COMPENG)*, Jul. 2022, pp. 1–5.

[23] K. D. Ballal, R. Singh, L. Dittmann, and S. Ruepp, "Experimental evaluation of roaming performance of cellular IoT networks," in *Proc. 13th Int. Conf. Ubiquitous Future Netw. (ICUFN)*, Jul. 2022, pp. 386–391.

[24] Z. Fang, J. Wang, J. Du, X. Hou, Y. Ren, and Z. Han, "Stochastic optimization-aided energy-efficient information collection in Internet of Underwater Things networks," *IEEE Internet Things J.*, vol. 9, no. 3, pp. 1775–1789, Feb. 2022.

[25] W. Wei, J. Wang, Z. Fang, J. Chen, Y. Ren, and Y. Dong, "3U: Joint design of UAV-USV-UUV networks for cooperative target hunting," *IEEE Trans. Veh. Technol.*, vol. 72, no. 3, pp. 4085–4090, Mar. 2023.

[26] E. F. Z. Santana, D. M. Bastista, and D. S. Milojicic, "SCSimulator: An open source, scalable smart city simulator," in *Proc. SBRC*, 2016, pp. 1–8.

[27] A. M. Del Esposte, E. F. Z. Santana, L. Kanashiro, F. M. Costa, K. R. Braghetto, N. Lago, and F. Kon, "Design and evaluation of a scalable smart city software platform with large-scale simulations," *Future Gener. Comput. Syst.*, vol. 93, pp. 427–441, Apr. 2019.

[28] M. El Soussi, P. Zand, F. Pasveer, and G. Dolmans, "Evaluating the performance of eMTC and NB-IoT for smart city applications," in *Proc. IEEE Int. Conf. Commun. (ICC)*, May 2018, pp. 1–7.

[29] G. of Canada Broadcasting and Telecommunications Regulation. (2022). *Spectrum Licenses Site Data*. [Online]. Available: http://sms-sgs.ic.gc.ca/eic/site/sms-sgs-prod.nsf/eng/h_00010.html

[30] (2022). *Portail Données Ouvertes Montreal*. [Online]. Available: https://donnees.montreal.ca/ville-de-montreal

[31] F. Malandra, H. Mellah, A. D. Firouzabadi, C. Wetté, and B. Sansò, "A layered and grid-based methodology to characterize and simulate IoT traffic on advanced cellular networks," *IEEE Internet Things Mag.*, vol. 6, no. 1, pp. 134–140, Mar. 2023.

[32] *Study on Channel Model for Frequencies From 0.5 to 100 GHz*, document TR 38.901, version 16.1.0, Sophia Antipolis, France, 3GPP, 2020. [Online]. Available: http://www.3gpp.org/DynaReport/38901.htm

[33] E. Dahlman, S. Parkvall, and J. Sköld, *4G, LTE-Advanced Pro and The Road to 5G*, 3rd ed. New York, NY, USA: Academic, 2016.

[34] *LTE; Evolved Universal Terrestrial Radio Access (E-UTRA) and Evolved Universal Terrestrial Radio Access Network (E-UTRAN); Overall Description; Stage 2*, document ETSI TS 136 300 V16.2.0 (2020-07), Route des Lucioles, Sophia Antipolis Valbonne, FR, Third Generation Partnership Project, Jan. 2020.

[35] G. Foddis, R. G. Garroppo, S. Giordano, G. Procissi, S. Roma, and S. Topazzi, "On RACH preambles separation between human and machine type communication," in *Proc. IEEE Int. Conf. Commun. (ICC)*, May 2016, pp. 1–6.

[36] *Universal Mobile Telecommunications System (UMTS);LTE; Feasibility Study for Evolved Universal Terrestrial Radio Access (UTRA) and Universal Terrestrial Radio Access Network (UTRAN)*, document ETSI TR 125 912 V16.0.0 (2020-09), Route des Lucioles, Sophia Antipolis Valbonne, FR, Third Generation Partnership Project, Jul. 2018.

[37] *LTE; Evolved Universal Terrestrial Radio Access (E-UTRA); Physical Channels and Modulation*, document ETSI TS 136 211 V16.6.0 (2021-08), Route des Lucioles, Sophia Antipolis Valbonne, FR, Third Generation Partnership Project, 2017.

[38] M. Z. Shafiq, L. Ji, A. X. Liu, J. Pang, and J. Wang, "A first look at cellular machine-to-machine traffic: Large scale measurement and characterization," *ACM SIGMETRICS Perform. Eval. Rev.*, vol. 40, no. 1, pp. 65–76, Jun. 2012, doi: 10.1145/2318857.2254767.

[39] *Study on RAN Improvements for Machine-Type Communications*, document 3GPP TR 37.868 V11.0.0, Route des Lucioles, Sophia Antipolis Valbonne, FR, Third Generation Partnership Project, Sep. 2011.

[40] F. Capozzi, G. Piro, L. A. Grieco, G. Boggia, and P. Camarda, "Downlink packet scheduling in LTE cellular networks: Key design issues and a survey," *IEEE Commun. Surveys Tuts.*, vol. 15, no. 2, pp. 678–700, 2nd Quart., 2013.

[41] *LTE; Evolved Universal Terrestrial Radio Access (E-UTRA); Physical Layer Procedures*, document ETSI TS 136 213 V16.9.0, Route des Lucioles, Sophia Antipolis Valbonne, FR, Third Generation Partnership Project, Feb. 2020.

[42] A. Asghar, H. Farooq, and A. Imran, "Outage detection for millimeter wave ultra-dense HetNets in high fading environments," in *Proc. IEEE Int. Conf. Commun. (ICC)*, May 2019, pp. 1–6.

[43] F. Chernogorov, J. Turkka, T. Ristaniemi, and A. Averbuch, "Detection of sleeping cells in LTE networks using diffusion maps," in *Proc. IEEE 73rd Veh. Technol. Conf. (VTC Spring)*, May 2011, pp. 1–5.

[44] E. Chu, I. Bang, S. H. Kim, and D. K. Sung, "Self-organizing and self-healing mechanisms in cooperative small-cell networks," in *Proc. IEEE 24th Annu. Int. Symp. Pers., Indoor, Mobile Radio Commun. (PIMRC)*, Sep. 2013, pp. 1576–1581.

[45] Y. Ma, M. Peng, W. Xue, and X. Ji, "A dynamic affinity propagation clustering algorithm for cell outage detection in self-healing networks," in *Proc. IEEE Wireless Commun. Netw. Conf. (WCNC)*, Apr. 2013, pp. 2266–2270.

[46] U. Masood, A. Asghar, A. Imran, and A. N. Mian, "Deep learning based detection of sleeping cells in next generation cellular networks," in *Proc. IEEE Global Commun. Conf. (GLOBECOM)*, Dec. 2018, pp. 206–212.

[47] O. Onireti, A. Zoha, J. Moysen, A. Imran, L. Giupponi, M. Ali Imran, and A. Abu-Dayya, "A cell outage management framework for dense heterogeneous networks," *IEEE Trans. Veh. Technol.*, vol. 65, no. 4, pp. 2097–2113, Apr. 2016.

[48] J. Turkka, F. Chernogorov, K. Brigatti, T. Ristaniemi, and J. Lempiäinen, "An approach for network outage detection from drive-testing databases," *J. Comput. Netw. Commun.*, vol. 2012, pp. 1–13, 2012.

[49] W. Xue, M. Peng, Y. Ma, and H. Zhang, "Classification-based approach for cell outage detection in self-healing heterogeneous networks," in *Proc. IEEE Wireless Commun. Netw. Conf. (WCNC)*, Apr. 2014, pp. 2822–2826.

[50] F. Chernogorov, S. Chernov, K. Brigatti, and T. Ristaniemi, "Sequence-based detection of sleeping cell failures in mobile networks," *Wireless Netw.*, vol. 22, no. 6, pp. 2029–2048, Aug. 2016.

[51] S. Chernov, F. Chernogorov, D. Petrov, and T. Ristaniemi, "Data mining framework for random access failure detection in LTE networks," in *Proc. IEEE 25th Annu. Int. Symp. Pers., Indoor, Mobile Radio Commun. (PIMRC)*, Sep. 2014, pp. 1321–1326.

[52] T. Omar, Z. Abichar, A. E. Kamal, J. M. Chang, and M. A. Alnuem, "Fault-tolerant small cells locations planning in 4G/5G heterogeneous wireless networks," *IEEE Trans. Veh. Technol.*, vol. 66, no. 6, pp. 5269–5283, Jun. 2017.

[53] A. Saeed, O. G. Aliu, and M. A. Imran, "Controlling self healing cellular networks using fuzzy logic," in *Proc. IEEE Wireless Commun. Netw. Conf. (WCNC)*, Apr. 2012, pp. 3080–3084.

[54] B. Cheung, S. Fishkin, G. Kumar, and S. Rao, "Method of monitoring wireless network performance," U.S. Patent App. 10 946 255, Mar. 23, 2006.

[55] O. G. Manzanilla-Salazar, F. Malandra, H. Mellah, C. Wetté, and B. Sansò, "A machine learning framework for sleeping cell detection in a smart-city IoT telecommunications infrastructure," *IEEE Access*, vol. 8, pp. 61213–61225, 2020.

[56] V. Therrien, H. Mellah, V. Boutin, and B. Sansò, "A large-scale simulator for NB-IoT," *IEEE Access*, vol. 10, pp. 68231–68239, 2022.

[57] L. Bastos, G. Capela, A. Koprulu, and G. Elzinga, "Potential of 5G technologies for military application," in *Proc. Int. Conf. Mil. Commun. Inf. Syst. (ICMCIS)*, May 2021, pp. 1–8.
[58] S. Wijethilaka and M. Liyanage, "Survey on network slicing for Internet of Things realization in 5G networks," *IEEE Commun. Surveys Tuts.*, vol. 23, no. 2, pp. 957–994, 2nd Quart., 2021.
[59] N. Abbas, Y. Zhang, A. Taherkordi, and T. Skeie, "Mobile edge computing: A survey," *IEEE Internet Things J.*, vol. 5, no. 1, pp. 450–465, Feb. 2018.
[60] C. K. Dehury, P. K. Donta, S. Dustdar, and S. N. Srirama, "CCEI-IoT: Clustered and cohesive edge intelligence in Internet of Things," in *Proc. IEEE Int. Conf. Edge Comput. Commun. (EDGE)*, Jul. 2022, pp. 33–40.
[61] J. G. Andrews, S. Buzzi, W. Choi, S. V. Hanly, A. Lozano, A. C. K. Soong, and J. C. Zhang, "What will 5G be?" *IEEE J. Sel. Areas Commun.*, vol. 32, no. 6, pp. 1065–1082, Jun. 2014.
[62] J. Liu, C.-H.-R. Lin, Y.-C. Hu, and P. K. Donta, "Joint beamforming, power allocation, and splitting control for SWIPT-enabled IoT networks with deep reinforcement learning and game theory," *Sensors*, vol. 22, no. 6, p. 2328, Mar. 2022.
[63] M. Z. Aslam, Y. Corre, E. Björnson, and E. G. Larsson, "Performance of a dense urban massive MIMO network from a simulated ray-based channel," *EURASIP J. Wireless Commun. Netw.*, vol. 2019, no. 1, Dec. 2019.

ABBAS DEHGHANI FIROUZABADI received the B.Sc. degree in electrical engineering from the K. N. Toosi University of Technology, Tehran, Iran, in 2011, and the M.Sc. and Ph.D. degrees in electrical engineering from the University of Tehran, Tehran, in 2014 and 2019, respectively. He is currently a Postdoctoral Fellow with Ecole Polytechnique de Montréal, where he is working on a 5G traffic simulator in a smart city. His research interests include the design, analysis, and optimization of wireless communication systems.

HAKIM MELLAH (Member, IEEE) received the B.E. and M.A.Sc. degrees in electrical engineering and the Ph.D. degree in electrical and computer engineering from Concordia University, Montréal, QC, Canada, in 1996, 1999, and 2018, respectively. He is currently a Postdoctoral Fellow with Ecole Polytechnique de Montréal. His research interest includes the machine quality of experience for the IoT applications in a smart city environment.

ORESTES MANZANILLA-SALAZAR (Member, IEEE) received the B.E. degree in production engineering and the M.A.Sc. degree in systems engineering from Simón Bolívar University (USB), Venezuela, in 2002 and 2005, respectively. He is currently pursuing the Ph.D. degree in electrical engineering with Polytechnique Montréal, Montréal, QC, Canada.

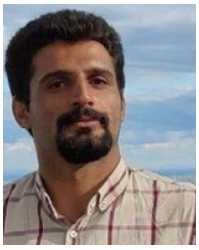

REZA KHALVANDI received the B.Sc. and M.Sc. degrees from the Sharif University of Technology, in 2014 and 2016, respectively. He is currently pursuing the Ph.D. degree with Polytechnique Montréal. His research interest includes large-scale solutions for distributed wireless networks.

VINCENT THERRIEN received the B.E. degree in electrical engineering from Polytechnique Montréal, Montréal, QC, Canada, in 2022. He is currently with the 3D sensor industry. His research interests include large-scale simulators and hardware acceleration.

VICTOR BOUTIN received the B.E. and M.A.Sc. degrees in electrical engineering from Polytechnique Montréal, Montréal, QC, Canada, in 2019 and 2021, respectively. He is currently with the robotics industry. His research interests include 5G technologies and large-scale simulators.

BRUNILDE SANSÒ (Senior Member, IEEE) is currently a Full Professor of telecommunication networks with the Electrical Engineering Department, Polytechnique Montréal, where she leads LORLAB, a research group dedicated to developing effective methods for the design and performance of wireless and wired telecommunication networks. She has been a consultant of operators, equipment manufacturers, and the mainstream media. She has published extensively in the telecommunication networks and operations research literature. Her current research interests include the performance, reliability, optimization of large-scale networks with stringent applications, and reducing their environmental impact. She has been a recipient of several awards and honors.